INTERNATIONAL JOURNAL OF AUTOMOTIVE AND MECHANICAL ENGINEERING
ISSN: 2229-8649 e-ISSN: 2180-1606
VOLUME 23, ISSUE 1, 2026, 13264 - 13277
DOI: https://doi.org/10.15282/ijame.23.1.2026.8.1006

RESEARCH ARTICLE

A hybrid entropy-VIKOR-Taguchi approach for sustainable optimization of diesel engine performance and emissions

Naseeb Khan[1], Jagadesh Kumar Jatavallabhula[2]*, Bridjesh Pappula[3], Vaddi Venkata Satyanarayana[2]

[1]Department of Mechanical Engineering, Shadan College of Engineering & Technology, Hyderabad, India.
[2]Department of Mechanical Engineering, Vidya Jyothi Institute of Technology, Aziznagar, Hyderabad, India.
[3]Department of Chemical & Materials Engineering, College of Science, Engineering and Technology, University of South Africa (UNISA), c/o Christiaan de Wet & Pioneer Avenue, Florida Campus 1710, Johannesburg, South Africa.

Abstract – The urgent demand for sustainable transport fuels highlights biodiesel-hydrogen dual-fueling as a promising pathway to improve engine efficiency while reducing carbon-based emissions. Nevertheless, optimizing combustion parameters to balance performance with stringent emission constraints remains a major challenge. This study introduces a hybrid Entropy-VIKOR-Taguchi framework to optimize the performance, combustion, and emission characteristics of a compression-ignition engine operating on a cottonseed biodiesel (B20)-hydrogen blend. The methodology integrates entropy-based weighting for objective parameter prioritization, VIKOR for compromise decision-making, and Taguchi design for efficient experimentation, thereby minimizing trial costs and enhancing reproducibility. Experiments evaluated three key parameters, namely injection pressure (200-240 bar), compression ratio (16.5-18.5), and hydrogen flow rate (10-20 L/min). Results showed that hydrogen enrichment improved combustion, with peak pressure reaching 85 bar and a maximum heat release rate of 86 J/deg. Engine efficiency increased to 33.52% BTE and a minimum BSFC of 0.213 kg/kWh, while emissions decreased (HC = 65 ppm, CO = 0.016%). However, NOx rose to 1380 ppm at high hydrogen flow, underscoring the trade-off between efficiency and emissions. The optimal condition, IP = 240 bar, CR = 17.5, and H_2 = 10 L/min, yielded the lowest VIKOR index (Q = 0.0588), ensuring balanced sustainability. This framework offers a transferable optimization pathway for dual-fuel engines, supporting decarbonization targets under SDG7 and SDG13.

Article History
Received : 27 September 2025
Revised : 16 December 2025
Accepted : 25 January 2026
Published : 12 March 2026

Keywords
VIKOR
Taguchi
Entropy
Emission
Biodiesel

1. Introduction

The rising demand for global energy is driven primarily by industrialization, urbanization, and population growth. In transport and industrial sectors, diesel engines continue to be the primary choice due to their reliability and long life, though they emit several pollutants like hydrocarbons (HC), oxides of carbon (CO_x), particulate matter (PM), oxides of nitrogen (NO_x), etc [1, 2]. Researchers and policymakers are interested in sustainable ways to reduce the environmental impact of diesel-powered applications, as their emissions are detrimental to the environment [3]. The need to mitigate greenhouse gas (GHG) emissions, along with a shift to sustainable energy solutions, is apparent in the progressive targets set by the United Nations (UN), the Intergovernmental Panel on Climate Change (IPCC), and the International Energy Agency (IEA). The Sustainable Development Goals (SDGs), including SDG 7 (Affordable and Clean Energy) and SDG 13 (Climate Action), also emphasize the need to decarbonize energy systems, enhance fuel efficiency, and adopt alternative sustainable energy sources[4, 5]. Biofuels, advanced ignition strategies, and engine design modifications have attracted attention for simultaneously enhancing diesel engine reliability and power while reducing emissions[6]. Sources of biodiesel include animal fats, non-food oils, and waste cooking oil. Biodiesel is non-toxic and biodegradable, and it emits lower emissions than diesel oil[7]. However, alternative approaches need to be developed to address ignition parameters and their challenges, such as fuel stability, reduced density energy, and NO_x emissions.

Governments and legislations introduced stronger emissions regulations, such as Euro 7 in Europe and Bharat Stage VI in India. There are regulations such as the Environmental Protection Agency (EPA) in America and China VI in China to reduce NOx, CO, and PM emissions[8, 9]. Stronger and regionally varying emission regulations are pushing diesel engines towards advanced after-treatment systems and low-carbon alternative fuels, supported by government incentives and policy measures worldwide. The European Union initiated the Renewable Energy Directive (RED II), which mandates an increase in the use of renewable fuels in transportation and provides tax incentives for biofuels and hydrogen production in the United States and India, and this is an example of a growing commitment to sustainable energy solutions[10]. The key sustainability challenges in diesel engines are fuel dependency, diesel combustion, and the trade-off between fuel economy and emissions[11]. Diesel engines depend on non-renewable petroleum-based fuels, which contribute to carbon emissions and climate change. Diesel combustion at elevated temperatures results in high NO_x and PM emissions, which are difficult to control without complex emission control strategies [12]. However, after-treatment methods such as EGR and catalytic converters decrease efficiency and increase the complexity and operating and maintenance costs of the engine. Furthermore, diesel engines face a trade-off between fuel economy and emissions, as improved combustion efficiency increases NOx formation, which is difficult to optimize for both performance and sustainability [13, 14].

Biodiesel has emerged as a viable renewable fuel for compression-ignition (CI) engines due to its oxygenated molecular structure, carbon neutrality, lower PM emissions, and its contribution to a circular economy [15]. The built-in

*CORRESPONDING AUTHOR | author | ✉ jagadeshkumar82@gmail.com

oxygen and typically higher cetane number improve fuel lubricity and promote more complete oxidation of intermediates, thereby reducing soot precursors and particulate matter and lowering lifecycle GHG emissions. At the same time, higher viscosity and altered volatility can deteriorate atomization, modify ignition delay, and alter local equivalence ratios, potentially increasing NO_x and imposing constraints on injection strategy and in-cylinder thermal management [16]. Hydrogen, by contrast, is a carbon-free energy carrier with very high laminar flame speed, wide flammability limits, and high diffusivity[17-19]. When supplied to a CI engine operating with a liquid pilot (diesel or biodiesel), a portion of the charge energy is stored in a premixed hydrogen-air mixture. This tends to accelerate combustion, increase the premixed heat-release fraction, and reduce HC and CO emissions due to improved oxidation [20-21]. However, the associated rise in local flame temperature and the steeper heat-release profile can intensify thermal NO formation via the extended Zeldovich mechanism if the hydrogen fraction and operating parameters are not carefully controlled[22-24]. In biodiesel-hydrogen dual-fuel operation, these effects interact: the oxygenated biodiesel pilot stabilizes autoignition and supports lower soot, while hydrogen enrichment accelerates burn and improves efficiency, but can drive NO_x peaks if peak temperature and residence time in high-temperature zones are excessive[17-18, 23]. Sustainable deployment, therefore, hinges on waste-derived biodiesel feedstocks that avoid land-use competition [22] and on dual-fuel strategies that exploit the complementary properties of biodiesel and hydrogen while actively managing NO_x through operating conditions and, where necessary, after-treatment[16, 23, 24].

Existing research has focused on biodiesel and diesel blends, or on hydrogen-enriched diesel combustion, as separate ways to increase the diesel engine's sustainability. Studies on biodiesel blends have reported reduced PM and CO emissions due to biodiesel's oxygenated molecular structure. Hydrogen enrichment in diesel engines has been shown to improve thermal efficiency but also to increase NO_x emissions due to higher combustion temperatures. Although each strategy can reduce emissions, the use of a dual-fuel approach, like biodiesel-hydrogen in a diesel engine, is limited. Critical research gaps remain in the simultaneous integration of biodiesel and hydrogen in a diesel engine. The application of hybrid multi-objective optimization techniques to systematically fine-tune engine parameters for combustion characteristics, emission reduction, and improvement in brake thermal efficiency. The development of a data-driven decision-making framework that prioritizes sustainability metrics while ensuring combustion stability. Optimization techniques, such as response surface methodology (RSM) [25], genetic algorithms (GA) [26], and artificial neural networks (ANN)[27], have been employed in combustion research. Nevertheless, these are frequently computationally intensive or involve experimental trials over a very long period. Furthermore, most of the research does not quantify the relative importance of emissions parameters in the decision-making process. To address such gaps, a new hybrid optimization method that is cost-effective in terms of experiments and at the same time effective in determining the best engine operating conditions is paramount. To address the above-mentioned research gaps, the current study proposes a hybrid optimization approach combining entropy weighting, the VIKOR method, and Taguchi design of experiments. The optimization of engine exhaust, performance, and combustion characteristics using sophisticated multi-criteria decision-making (MCDM) methods has not received much attention. The objectives of the present work are to investigate the role of IP, CR, and H_2 induction rate on the behavior of the emission and the general performance and combustion pattern of a diesel engine under the conditions of a cottonseed oil biodiesel (B20) and hydrogen mixed fuel, to develop a multi-objective optimization strategy for minimizing NO_x, HC, and CO emissions while maintaining combustion efficiency, to apply a hybrid method of integrating entropy weights, the VIKOR Method and the Taguchi technique to rank the combined engine emission responses and engine performance metrics and to establish a data-driven framework for optimizing biodiesel-hydrogen combustion.

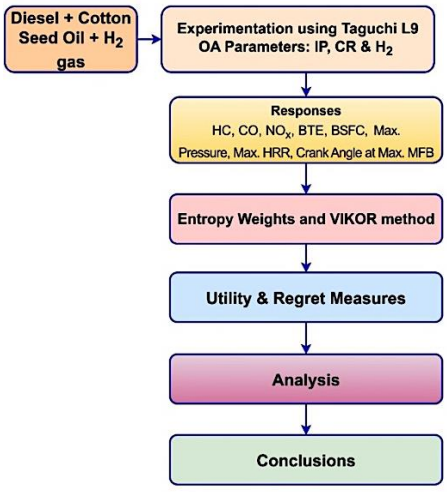

Figure 1. Flowchart of the research

This research integrates three advanced optimization techniques to enhance decision-making in sustainable diesel engine operation. Entropy weighting method quantitatively determines the relative significance of responses based on their variability across experimental trials. VIKOR Method: Unlike conventional MCDM approaches, VIKOR accounts for trade-offs among competing objectives, ensuring balanced optimization of performance and emissions. Taguchi

Experimental Design: The Taguchi method systematically reduces the number of trials by implementing orthogonal arrays (OA), ensuring efficient parameter optimization with minimal resource consumption. This approach enhances experimental efficiency compared to full factorial designs. This integrated methodology provides a practical, computationally efficient framework for optimizing biodiesel-hydrogen combustion conditions in diesel engines. Structured as follows, the remaining portion of this paper is structured as follows. Section 2 presents experimental methodology, including engine specifications, fuel properties, and test conditions. Section 3 describes the results and demonstrates the parameter contributions. Section 4 concludes the study and provides recommendations for future research. Figure 1 depicts a schematic flowchart of the current investigation, summarizing the workflow and experimental process.

2. Materials and Methods

2.1 Experimental Details

The engine used in this study is a Kirloskar TV-1 type, single-cylinder, four-stroke, water-cooled, single-acting, diesel engine (Figure 2), coupled with computer interfacing for all accessories to measure performance, combustion, and emission characteristics. The engine specifications are given in Table 1. Data acquisition of the selected responses is performed using LabVIEW software from National Instruments Corporation. Before testing, all key instruments were calibrated to ensure traceable and repeatable measurements. The eddy-current dynamometer was calibrated using a torque arm and certified dead weights; the indicated torque was adjusted to keep deviations from the reference within ±1 %. Engine speed was cross-checked against an independent digital tachometer at multiple set points. Exhaust emissions were monitored using a multi-gas analyzer and a smoke meter. Before each batch of tests, the analyzer was zeroed on clean gas and spanned with certified calibration mixtures for NO_x, HC, and CO, while the smoke meter was zeroed in filtered air. Each operating condition was repeated five times, and the reported performance, combustion, and emission values are the mean of these repeats.

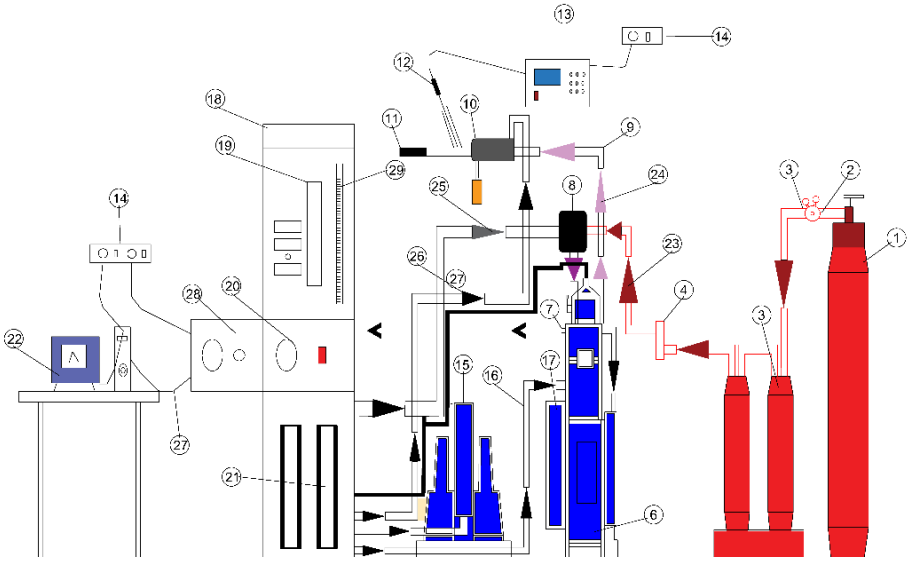

1. H_2 Cylinder, 2. H_2 Regulators, 3. Flashback arrestor, 4. Flame arrestors, 5. H_2 Flow meter, 6. Engine, 7. Cylinder pressure sensor, 8. Mixing chamber, 9. Exhaust flow pipe, 10. Calorimeter, 11. Exhaust gas to the atmosphere, 12. Exhaust gas analyzer probe, 13. Exhaust gas analyzer, 14. Power supply, 15. Eddy current dynamometer, 16. Engine water inlet pipeline, 17. Flywheel, 18. Fuel tank, 19. U-Tube manometer, 20. Loading unit, 21. Rotameters, 22. Computer, 23. H_2 gas flow pipe, 24. Exhaust gas, 25. Air supply, 26. Calorimeter water inlet, 27. NI-6210 USB Multifunction line, 28. Control panel, 29. Burette.

Figure 2. Schematic view of experimental setup

Table 1. The specifications of the engine

Type of ignition	Compression ignition
Rated Power (kW)	3.5
Dynamometer	Eddy Current Type
Fuel Injection	Direct Injection
Piston Bowl	Hemispherical
Stroke (mm)	110
Speed (rpm)	1500
Cylinder Capacity (cc)	661
Bore (mm)	87.5
Connecting Rod Length (meter)	0.234
Injection Timing (degree BTDC)	23

2.2. Fuels Used

Diesel, cottonseed oil, and hydrogen (H_2) fuels are used in the present investigation. Table 2 provides the properties of the various fuels. The use of cottonseed oil as a test fuel is motivated by sustainability factors, as it is produced from non-edible, waste-derived feedstocks, reducing the carbon footprint associated with traditional diesel burning [28]. Cottonseed oil properties were obtained from the supplier's certified technical data sheet, which is based on standard ASTM/EN test methods and quality-controlled measurements, and these values were cross-checked against ranges reported in the literature. H_2 is preferred due to its zero emissions during combustion and its potential to improve the sustainability of diesel engines in terms of carbon emissions [29]. The combination of both fuels has ecological significance and provides a low-emission, highly efficient alternative to diesel engines [30]. Cottonseed oil and diesel are blended at a 20:80 ratio and introduced into the cylinder near the end of the suction stroke. H_2 is introduced separately through a port and into the cylinder during the suction stroke. In all tests, H_2 was supplied as dry gas directly from the high-pressure cylinder through pressure regulation. Adding H_2 can reduce emissions and increase combustion efficiency, but it faces technological challenges. The low ignition energy, along with H_2 high flame speed, requires precise control to prevent combustion instabilities and NO_x formation. To overcome these challenges, a flow rate of 10-20 LPM was identified as optimal based on previous research findings and engine operating conditions [30, 31]. All experiments were conducted with specific safety measures for H_2 storage and delivery. H_2 was stored at 150 bar in certified cylinders. The supply line to the engine was equipped with a pressure regulator in two stages and fitted with non-return valves, flashback arrestors, and flame arrestors, as indicated in Fig. 2. Before each test session, the complete hydrogen circuit was checked for leaks using a soap-solution test, and the laboratory doors and windows were kept open to prevent accumulation of H_2. An emergency shut-off valve was installed upstream of the flow control unit to allow immediate isolation of the hydrogen supply in the event of an abnormal operating condition.

Table 2. Properties of the fuels employed

Property	Diesel fuel	H_2	Cottonseed oil	B20
Specific Gravity @ 15ºC kg/m^3	0.830	0.0838	0.913	0.867
Cloud point (ºC)	4	---	6	5
Kinematic viscosity (mm^2/s) @ 40ºC	2.64	110	31.35	3.47
Flash point (ºC)	71	---	195	90
Cetane Index	47	---	52	
Calorific Value (MJ/kg)	43	119.93	39.16	41.46
Pour point (ºC)	-6	---	-4	-3
Fire point (ºC)	85	---	220	98

Table 3. The factors selected and levels used

Factor	Notation	Units	Levels of the factors		
			Low (-1)	Medium (0)	High (1)
Injection Pressure	IP	bar	200	220	240
Compression Ratio	CR	-	16.5	17.5	18.5
Hydrogen	H_2	lpm	10	15	20

Table 4. Parameters and the Coded values

Run	Absolute Values			Coded Values		
	IP	CR	H_2	IP	CR	H_2
1	200	16.5	10	-1	-1	-1
2	200	17.5	15	-1	0	0
3	200	18.5	20	-1	1	1
4	220	16.5	15	0	-1	0
5	220	17.5	20	0	0	1
6	220	18.5	10	0	1	-1
7	240	16.5	20	1	-1	1
8	240	17.5	10	1	0	-1
9	240	18.5	15	1	1	0

2.3. Taguchi Method

The full factorial design is accurate and has a high resolution, but it is also tedious, time-consuming, and expensive to run. In this work, the L9 array was selected because it provides an acceptable balance between efficiency and accuracy. The study improved result consistency by repeating each experiment and then calculating the average of the top two results for reporting [32]. Injection pressure (IP), compression ratio (CR), and H_2 flow rate are treated as three factors, each at three levels, in the present investigation, as shown in Table 3. Adding H_2 can reduce emissions and improve combustion efficiency, but it also poses technological challenges. The low ignition energy, wide flammability limits, and high flame speed of H_2 require precise control to avoid backfire, knocking, and excessive NO_x formation. The hydrogen

flow rates were therefore constrained to 10, 15, and 20 lpm. In the present investigation, the Taguchi method is employed for experimentation with three different factors whose combinations are presented in Table 4.

2.4. Responses Measured

The responses in the present study are (i) emissions from the engine, viz., HC, CO, and NO_x ; (ii) performance of the engine, viz., BTE and BSFC; (iii) combustion characteristics, viz., maximum in-cylinder pressure, crank angle at which the maximum mass fraction burnt, and net HRR. These are recorded for the purpose of analyzing and thereby optimizing the parameters to obtain comprehensive sustainability. Cylinder pressure was recorded at a crank-angle resolution of 0.5°CA over 100 consecutive cycles under steady-state conditions and ensemble-averaged before analysis. The net rate of heat release was then calculated using a single-zone first-law model and smoothed in the crank-angle domain with a 5-point moving-average filter to suppress high-frequency noise while preserving combustion phasing. The test rig used to measure responses is prone to random uncertainty, and the percentage magnitude of this uncertainty is presented in Table 5.

Table 5. Uncertainty analysis

Parameter Category	Name of the parameter	Max. error	Uncertainty (%)
Performance related	Brake power (kW)	0.065	± 1.8%
	Compression ratio	0.01817	± 0.103%
	BSFC (kg/kWh)	1.383×10^{-3}	± 0.53%
	BTE (%)	0.232	± 0.713%
	Fuel consumption (kg/h)	9.7×10^{-3}	± 1.06%
Combustion related	Cylinder pressure (bar)	0.018	± 0.02%
	Net HRR (J/deg)	0.2037	± 0.385%
	Mass fraction burned (%)	0.605	± 0.676%
	Rate of pressure rise (dp/dθ)	0.254	± 0.44%
Total uncertainty			± 3.84%

2.5. Entropy Weight

In the context of information theory, entropy measures how unpredictable a source is, meaning how much information it can reveal. The probability of each outcome is used as its weight when calculating the total information [33]. The response and the number of experiments are taken into account when calculating the weights. In the present study, m = 9 and n = 8 responses were adopted for the experiments. Weights and entropy are obtained using Eqs. (1-3).
First, the results are converted into p-values using Eq. (1).

$$p_{ij} = \frac{x_{ij}}{m+\sum_{i=1}^{m} x_{ij}^2} \tag{1}$$

where, $x_{ij}$is the magnitude of the response and $i = 1, 2, \ldots . m$ and $j = 1, 2, \ldots . n$.
From here, the entropy value for each indicator is calculated using Eq. (2).

$$e_j = -\sum_{i=1}^{m}\left[p_{ij} \times \ln\left(p_{ij}\right)\right] - \left[1 - \sum_{i=1}^{m} p_{ij}\right] \times \ln\left(1 - \sum_{i=1}^{m} p_{ij}\right) \tag{2}$$

The final weights for each indicator are determined using Eq. (3).

$$w_j = \frac{1-e_j}{\sum_{j=1}^{m}(1-e_j)} \tag{3}$$

2.6. VIKOR method

The VIKOR approach can be applied to multi-response decision-making by following a defined sequence of steps. The alternative associated with the lowest VIKOR index is then identified as the optimal solution. The results are converted into the decision matrix, i.e., $D[x_{ij}]_{m\times n}$, where D is the decision matrix and x_{ij} is the j[th] attribute's results of the i[th] alternative. The decision matrix can be expressed as mentioned in Eq. (4).

$$D = \begin{bmatrix} x_{11} & x_{12} & \ldots & x_{1n} \\ x_{21} & x_{22} & \ldots & x_{2n} \\ x_{31} & x_{32} & \ldots & x_{3n} \\ \vdots & \vdots & \vdots & \vdots \\ x_{m1} & x_{m2} & \ldots & x_{mn} \end{bmatrix} \tag{4}$$

where i = 1,2,3,4, …, m & j = 1,2,3,4, …., n

The decision matrix is normalized using Equations (5) and (6) to maximize and minimize the output responses, respectively.

$$n_{ij} = \frac{x_{ij} - \min\left(x_{ij}\right)}{\max(x_{ij}) - \min\left(x_{ij}\right)} \tag{5}$$

$$n_{ij} = \frac{\max(x_{ij}) - x_{ij}}{\max(x_{ij}) - \min\left(x_{ij}\right)} \tag{6}$$

where i = 1,2,3,4,…m & j = 1,2,3,4,….n
Calculate the utility measure Si values according to Eq. (7).

$$S_i = \sum_{j=1}^{n}(w_j n_{ij}) \tag{7}$$

where w_j is weight associated with the j^{th} criterion.
Calculate the regret measure R_i values using Eq. (8).

$$R_i = \max\left[w_j n_{ij}\right] \tag{8}$$

The VIKOR indices are computed using the sensitivity factor $\vartheta = 0.5$ employing Eq. (9).

$$Q_i = \vartheta \frac{S_i - \min S_i}{\max S_i - \min S_i} + (1-\vartheta)\frac{R_i - \min R_i}{\max R_i - \min R_i} \tag{9}$$

The compromise parameter ϑ in the VIKOR method was set to $\vartheta = 0.5$ in the baseline analysis, representing an equal balance between group utility and individual regret. To examine the robustness of the ranking, additional calculations were performed for $\vartheta = 0.25$ and $\vartheta = 0.75$.

3. Results and Discussion

The experimentation was carried out using various fuel combinations, viz., pure diesel, B20, and H_2 gas, at different load conditions. In this pursuit, injection pressure and compression ratio have been varied for the fuels under consideration, and the results have been recorded. Figures 3-5 show typical samples of experimental results at 17.5 CR and 200 bar IP. Figure 3 illustrates the variation of BTE and BSFC with brake power, showing that BTE increases with H_2 while BSFC decreases at different load conditions. Figure 4 illustrates the variation in HC, CO, and NO_x emissions with engine load as more H_2 is added to the cylinder: CO and HC emissions decrease, while NO_x emissions increase. Figure 5 illustrates the combustion characteristics during engine operation. The net heat release rate (HRR) is lowest with B20 fuel because it operates under lean combustion conditions, which results in a lower energy density [23]. In the mass fraction burnt curve, with increasing H_2, the ignition delay decreased, and this change is reflected in the maximum pressure developed in the engine [24]. The curve is shifted to the left, reducing the crank angle from TDC during these combustion conditions.

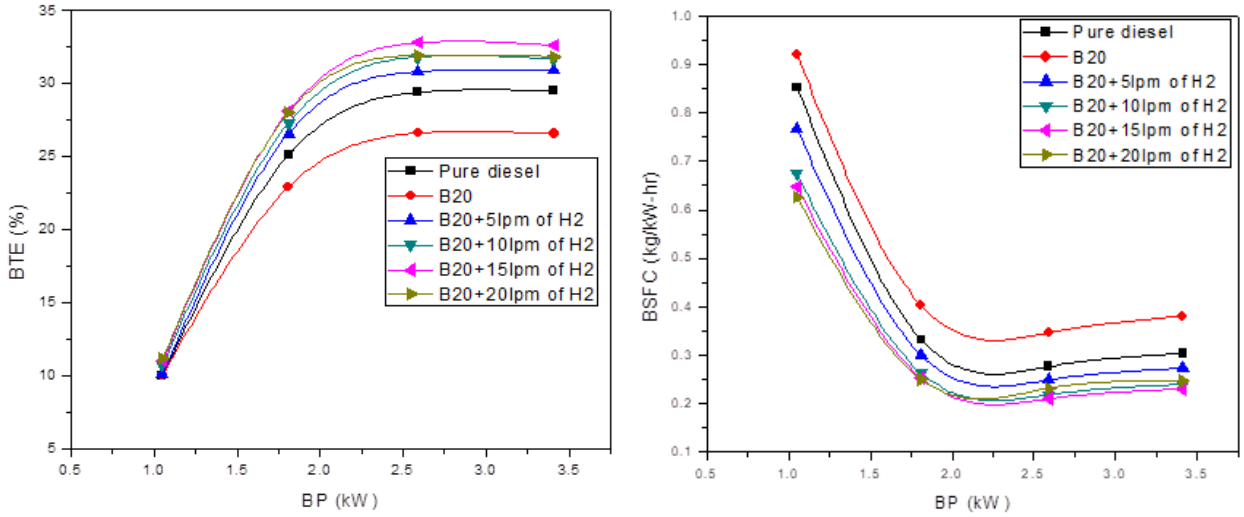

(a) (b)

Figure 3. Variation of performance of engine at 200 bar and 17.5 CR, (a) BTE vs BP, (b) BSFC vs BP

The NO_x trends can be interpreted in terms of the thermal pathway described by the extended Zeldovich mechanism, which is strongly governed by local flame temperature and high-temperature residence time[14]. Higher injection pressure and compression ratio both raise in-cylinder temperature and pressure, so at a given load, they increase the peak burned-gas temperature and extend the period during which the gas resides above about 2000 K, thereby promoting thermal NO formation [21]. Hydrogen enrichment further steepens the premixed heat release and increases the adiabatic flame temperature of the charge, so moderate H_2 flow rates can still be compatible with acceptable NO_x levels, whereas the highest H_2 level produces a sharp rise in NO_x despite improvements in HC and CO. The observed behavior is therefore consistent with a thermal-NO-dominated mechanism, where the efficiency gains from faster combustion and better oxidation are offset by the exponential sensitivity of NO_x to temperature as the operating point is pushed towards the upper end of the selected IP-CR-H_2 window [23]. The objective of this investigation is to identify the optimal parameter combination that yields overall sustainability and ultimately provides a comprehensive solution for all responses. Hence, the experimentation is now restricted to a Taguchi design using the L9 orthogonal array, with the input parameters IP, CR, and the volume of H_2 gas injected into the cylinder. The results for all runs at 75% engine load are presented in Table 6.

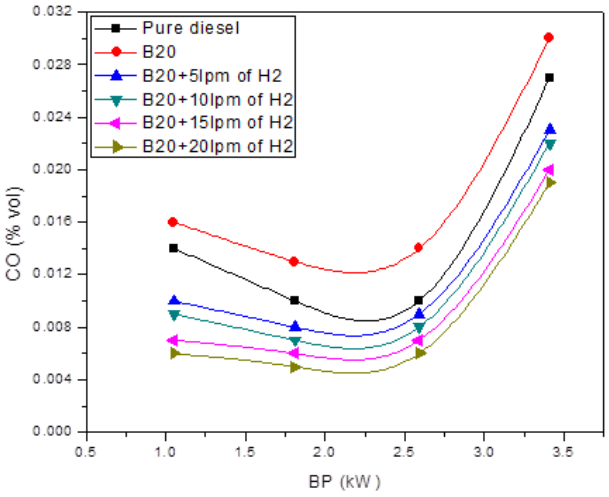

(a) CO vs BP

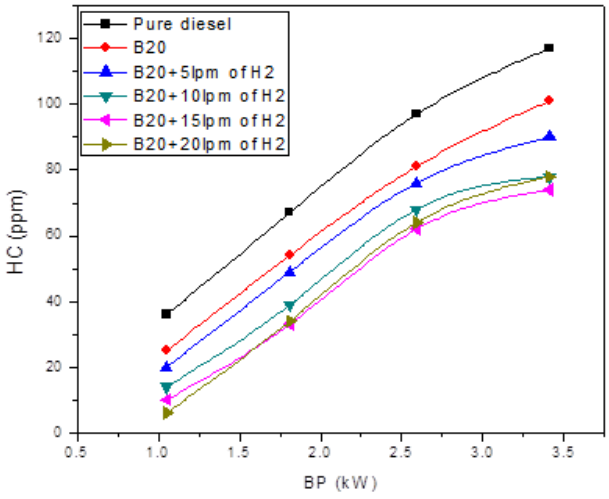

(b) HC vs BP

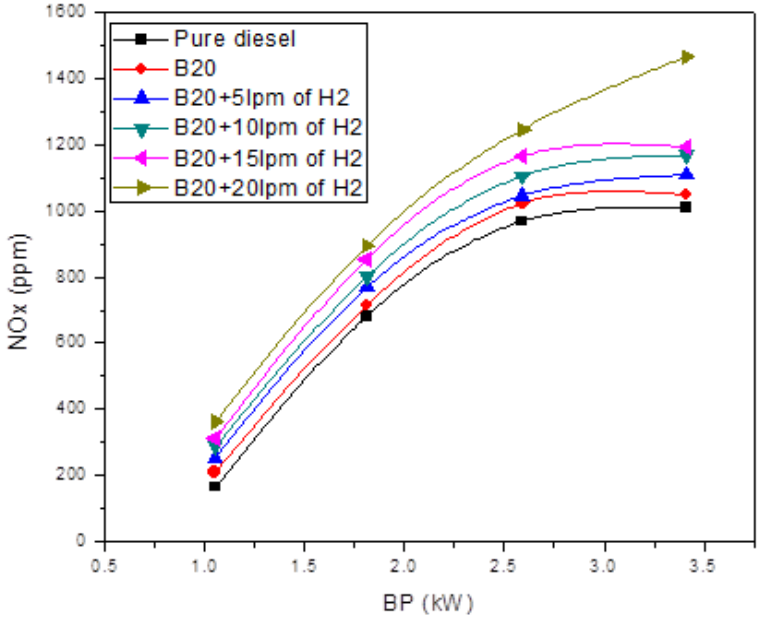

(c) NO_x vs BP

Figure 4. Variation of emissions of the engine at 200 bar and 17.5 CR

Table 6. Results of the investigation

Run	Emission Characteristics			Performance		Combustion Characteristics		
	HC (PPM)	CO (% VOL)	NO_x (PPM)	BTE (%)	BSFC (kg/kWh)	Max. Pressure (bar)	Max. HRR (J/deg)	Crank Angle at Max. MFB (º)
1	68	0.019	1100	28.50	0.215	69	65	21
2	73	0.0185	1185	32.60	0.230	80	69	23
3	74	0.021	1350	30.27	0.234	84	85	20.8
4	58	0.017	1300	30.24	0.213	82	69.5	21.5
5	72	0.0195	1375	33.52	0.251	85	69.7	20
6	79	0.0191	1250	30.90	0.235	77	86	21.2
7	65	0.016	1380	28.90	0.224	79	69.8	20.5
8	80	0.0235	1175	31.90	0.245	75	72	20.8
9	78	0.0215	1290	31.30	0.221	84	85.5	20.9

The fuel inducted into the cylinder is a mixture of pure diesel, cottonseed oil, and hydrogen gas. In run 3, the maximum pressure developed in the engine is 85 bar, with the parameters being an injection pressure (IP) of 220 bar, a compression ratio (CR) of 17.5, and hydrogen induction at 20 liters per minute (lpm); meanwhile, in run 6, the maximum heat release rate is found to be 86 J/deg. The recorded crank angle for the maximum mass fraction burnt in the cylinder ranges from 20 to 23 degrees from top dead center. Higher HRR increases cylinder pressure and results in increased power output, but it also increases the formation of pollutants, especially NO_x and soot. A higher mass fraction burned in the cylinder increases the pressure generated, which, in turn, leads to greater power output [30]. In addition to biodiesel and hydrogen,

the combustion rate increases due to the higher oxygen content and lower fuel viscosity [23]. The engine performance was quantified using BTE and BSFC across the tested operating conditions. Overall, BTE ranged from 28.6% to 33.52%, whereas BSFC ranged from 0.213 to 0.251 kg/kWh. The lowest BTE (28.6%) occurred when all control parameters were set to their minimum values, namely an IP of 200 bar, a CR of 16.5, and an H_2 flow rate of 10 L/min. Conversely, the BTE and BSFC peaks of 33.52 percent and 0.251 kg/kWh, respectively, were achieved at an IP of 220 bar, a CR of 17.5, and a H_2 flow rate of 20 L/min. In the context of fuel economy, the lowest BSFC (0.213 kg/kWh) occurred at the intermediate IP, and H_2 induction levels (220 bar and 15 L/min, respectively), and the CR level was kept at its low level (16.5). These trends suggest that the same set of operating parameters may not optimize BTE and BSFC, and that the interaction between H_2 enrichment and IP and CR is non-linear.

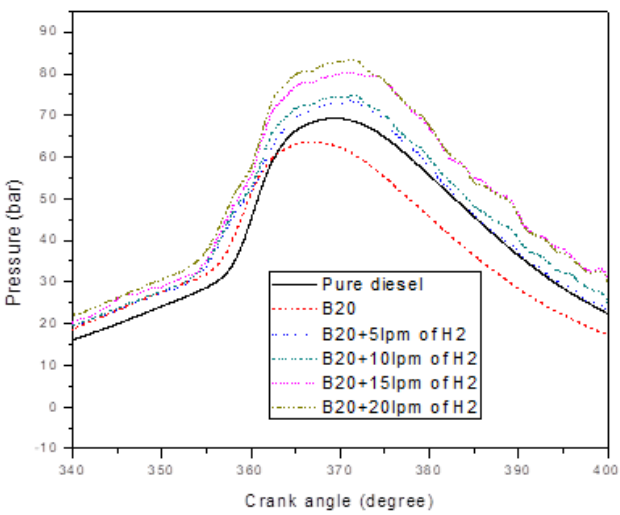

(a) CO vs BP

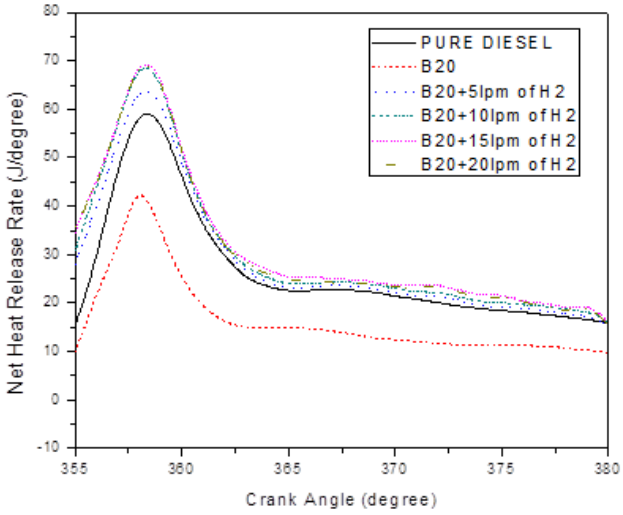

(b) HC vs BP

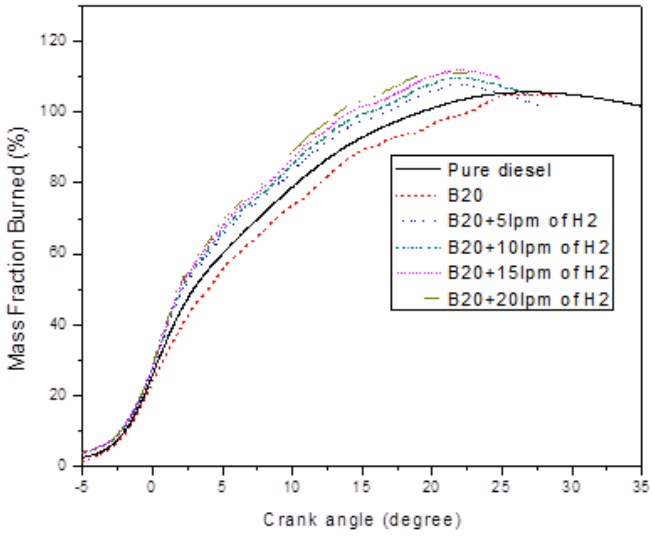

(c) NO_x vs BP

Figure 5. Variation of combustion characteristics of the engine at 200 bar and 17.5 CR

HC emissions are caused by incomplete combustion and fuel-rich areas within the cylinder [34]. HC emission (65 ppm) was lowest at IP = 240 bar, CR = 16.5, and H_2 =20 L/min (Run 7). This is because fuel atomization is better at higher injection pressure, enabling more complete combustion [35]. Conversely, the HC emission peak (80 ppm) occurred at IP = 240 bar, CR = 17.5, and H_2 = 10 L/min (Run 8), suggesting that a moderate compression ratio with decreased hydrogen induction could have led to incomplete oxidation, thereby raising HC emissions. Direct measurement of CO is through the incomplete oxidation of carbon in the fuel-air mixture. The minimum CO emission (0.016) was measured at an IP of 240 bar with a CR of 16.5 and a hydrogen flow rate of 20 L/min (Run 7), in accordance with the trend observed in the HC emissions. This implies that IP and hydrogen (H_2) enrichment favor full combustion, thereby lowering CO emissions [36]. The largest CO emission of 0.0235 was recorded at an IP of 240 bar, a CR of 17.5, and an H_2 flow rate of 10 L/min (Run 8), which was probably due to incomplete hydrogen oxidation and fuel stratification. The factors that mainly determine NOx emissions include combustion temperature and oxygen concentration. Optimal NO_x emission (1380 ppm) was observed in IP = 240 bar, CR = 16.5, and H_2 = 20 L/min (Run 7). This might be attributed to greater NOx production due to higher adiabatic flame temperature, resulting from hydrogen enrichment and leading to high in-cylinder temperatures [37]. Conversely, the minimum NO_x emission (1100 ppm) corresponded to the IP = 200 bar, CR =

16.5, and H_2 = 10 L/min (Run 1). This indicates that the injection pressure is reduced and the hydrogen induction is minimal, thereby achieving lower peak temperatures and reducing the formation of NO_x thermally [38].

The observed HC and CO trends can be understood in terms of global equivalence ratio and in-cylinder mixture formation at 75% load. For the B20 baseline, the higher liquid fuel flow and relatively lower degree of premixing lead to locally rich pockets near the spray core and the walls, promoting incomplete oxidation and, hence, higher HC/CO. Introducing hydrogen at moderate flow rates slightly leans the overall mixture for the same brake power and, together with higher injection pressure, improves spray atomization and air-fuel mixing, reducing wall wetting and enhancing oxidation of unburnt hydrocarbons and CO [31]. At the highest hydrogen flow and extreme settings of injection pressure or compression ratio, however, the charge can become more stratified again, with very reactive zones near the pilot spray and cooler regions near the boundaries, so residual rich pockets and locally quenched zones can still sustain HC/CO levels despite the overall leaner global equivalence ratio[39]. At constant IP and hydrogen flow, CR shows a clear and monotonic influence on performance and emissions. For example, at IP = 220 bar and H_2 = 15 L/min, increasing CR from 16.5 to 17.5 raises BTE and lowers BSFC, reflecting improved thermodynamic efficiency due to higher peak pressure and temperature. A further increase to CR = 18.5 produces only a marginal gain in BTE but leads to a noticeable increase in NO_x, indicating that the additional temperature rise mainly strengthens thermal-NO formation rather than improving useful work. Similar trends are observed at the other IP-H_2 combinations, confirming that CR primarily acts as an efficiency lever with a strong penalty on NOx beyond an intermediate optimum [11]. Table 7 presents the normalized values of the recorded responses. Under these parameter conditions, a divergent influence on the responses is observed; therefore, they are analyzed using a hybrid method that applies entropy weights, and the utility values are calculated using VIKOR indices. The higher-the-better criterion is employed for BTE, max. pressure, and HRR, while the lower-the-better criterion is employed for the responses BSFC, HC, CO, NO_x, and crank angle for maximum MFB [38, 39]

Table 7. Normalized results of the investigation

Run	HC	CO	NO_x	BTE	BSFC	Max. Pressure	Max. HRR	Crank Angle at Max. MFB
1	0.5455	0.6000	1.0000	0.0000	0.9375	0.0000	0.0000	0.6667
2	0.3182	0.6667	0.6964	0.8167	0.4688	0.6875	0.1905	0.0000
3	0.2727	0.3333	0.1071	0.3526	0.3437	0.9375	0.9524	0.7333
4	1.0000	0.8667	0.2857	0.3466	1.0000	0.8125	0.2143	0.5000
5	0.3636	0.5333	0.0179	1.0000	0.9375	1.0000	0.2238	1.0000
6	0.0455	0.5867	0.4643	0.4781	0.3125	0.5000	1.0000	0.6000
7	0.6818	1.0000	0.0000	0.0797	0.6563	0.6250	0.2286	0.8333
8	0.0000	0.0000	0.7321	0.6773	0.0000	0.3750	0.3333	0.7333
9	0.0909	0.2667	0.3214	0.5578	0.7500	0.9375	0.9762	0.7000

Table 8. Entropy and Weights of Responses

S. No	Parameter	Entropy	Weight
1	HC	0.1030	0.1481
2	CO	0.1385	0.1422
3	NO_x	0.0081	0.1638
4	BTE	0.2133	0.1299
5	BSFC	0.9920	0.0013
6	Max. Pressure	0.0949	0.1494
7	Max. HRR	0.0995	0.1487
8	Crank Angle at Max. MFB	0.2942	0.1165

Table 9. Utility, Regret, and VIKOR Indices

Run	Utility Measure (S)	Regret Measure (R)	VIKOR Index (Q)
1	0.4088	0.1638	0.5279
2	0.4938	0.1141	0.2677
3	0.5188	0.1416	0.6153
4	0.5761	0.1481	0.8425
5	0.5630	0.1494	0.8191
6	0.5221	0.1487	0.6958
7	0.4789	0.1422	0.5093
8	0.3989	0.1199	0.0588
9	0.5443	0.1451	0.7230

Table 8 presents the entropy values and corresponding weights assigned to each response based on their variability and significance in the optimization process (Eqs. (1-3)). The entropy-weighted method objectively measures how much each emission parameter contributes to the overall disorder in the data. The results indicate that NO_x emissions have the greatest weight (0.1638), indicating their dominant influence on the engine's emission characteristics, followed by HC (0.1481) and CO (0.1422). This order implies that NO_x emissions exhibit the greatest variability and sensitivity to changes in engine parameters and should be given priority in optimization. This means that the impact of CO is relatively less but

still significant, and HC is in an intermediate position. These conclusions inform the VIKOR method on how to capture the optimal compromise solution for emission reduction, ensuring a balanced trade-off among all emission constituents. The utility, regret, and VIKOR indices have been calculated using Eqs. (7-9) and are given in Table 9.

The sensitivity factor ϑ is varied with three values, namely, 0.25, 0.5, and 0.75, to compute the VIKOR indices. In all three cases, the alternative corresponding to IP = 240 bar, CR = 17.5, and H_2 = 10 L/min remained the best or near-best compromise solution, indicating that the final choice is insensitive to reasonable variations in ϑ. In this study, the VIKOR index is treated as a composite sustainability-oriented metric that aggregates multiple, partly conflicting responses into a single objective. Following common practice in Taguchi and multi-criteria optimization, Analysis of Variance (ANOVA) is applied to this scalar index as a heuristic sensitivity tool to quantify the relative contributions of injection pressure, compression ratio, and hydrogen flow to the combined performance-emission goal, rather than as a replacement for ANOVA on individual physical responses. The ANOVA results for the VIKOR indices are also shown in Table 10, which indicates the proportions of each engine parameter in the response characteristics. The strongest influence is shown by IP (42.50), indicating it has a dominant effect on emission behavior, especially on NOx formation, as it directly influences combustion temperature and pressure [40]. CR makes a moderate contribution of 28.07, indicating a moderate effect on atomization quality and combustion efficiency, which impacts HC and CO emissions. H_2 has the least influence (12.66%). However, it is still a critical component of combustion enhancement and emission control.

Table 10. ANOVA of VIKOR indices

Source	DF	SS	MS	F-Value	Contribution (%)
IP	2	0.22747	0.11373	3.08	42.50
CR	2	0.15024	0.07512	2.03	28.07
H_2	2	0.08363	0.04181	1.13	15.63
Error	2	0.07387	0.03693	--	--
Total	8	0.53521	--	--	--

Figure 6 is the Analysis of Means (ANOM) plot of the VIKOR indices, which visually illustrates the impact of IP, CR, and H_2 on overall emissions optimization. The VIKOR index was evaluated using the lower-the-better criterion; that is, the best combination of parameters yields the lowest Q value, i.e., the best trade-off among all responses. The combination that performed best, i.e., IP = 240 bar, CR = 17.5, and H_2 = 10 L/min, was identified as the most desirable for minimum emissions and optimal engine performance. The ANOM confirms the robustness of the IP tuning in the optimization of the diesel engine based on sustainability and the success of the Entropy VIKOR Taguchi framework in selecting an optimal multi-objective solution [41-43]. These operating conditions result in an optimality condition and increased sustainability of the experimental matrix and of general sustainability, due to the increased BP and reduced emissions.

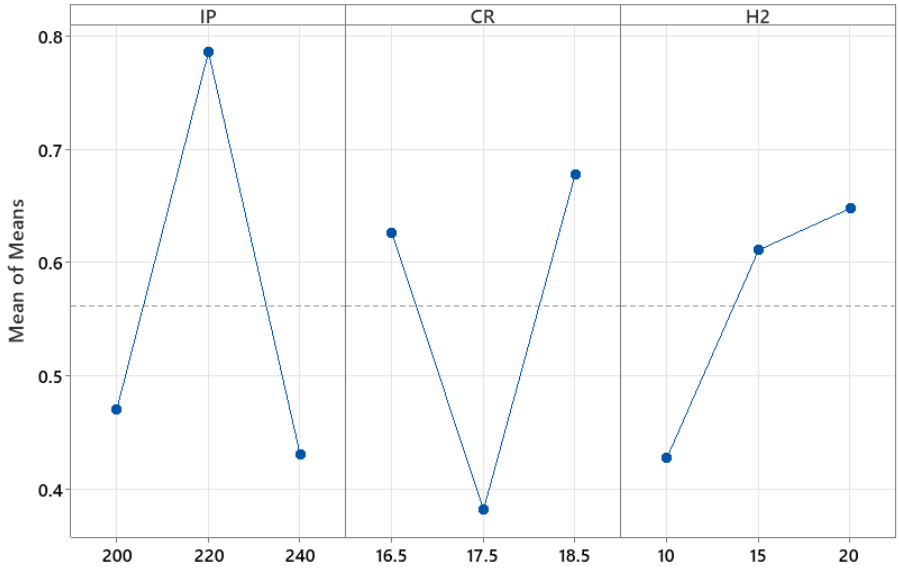

Figure 6. ANOM plot of the VIKOR Indices

The optimal parameter condition arrived at by the hybrid methodology (IP = 240 bar, CR = 17.5, H_2 = 10 L/min) coincides with experimental Run 8 in the L9 array. Therefore, the performance, combustion, and emission values reported for this optimum are based on direct experimental measurements and not extrapolated predictions. The optimal condition is therefore internally validated within the Taguchi design, and no separate confirmatory run outside the array is required. The predicted optimal value = $T + \sum_{i=1}^{n}(T_i - \mathrm{T})$ where T is the overall mean and T_i is the mean of the i^{th} parameter at optimal condition, given by 0.50625 + (0.43125 − 0.50625) + (0.39375 − 0.50625) = 0.2375.

95% confidence interval for the predicted optimal value at (2, 2) degrees of freedom is found by the formula $\sqrt{\frac{F \times MSE}{n_e}}$ where F is the Fisher ratio, MSE is the mean square error, and n_e is the effective sample size. The interval is found to be within the limits 0 and 0.5104. The confirmation experiment is the Run-8 itself, and its VIKOR index is 0.0588, which lies within the computed confidence interval, confirming the accuracy of the model.

Recent work has explored hydrogen-enriched operation with various biodiesel feedstocks, including water hyacinth and Mesua ferrea biodiesel [20], RCCI concepts with hydrogen-enriched biofuels [21], cashew nut shell oil biodiesel/hydrogen dual-fuel engines optimized using response surface methodology [23], and hydrogen-assisted combustion with rapeseed/waste cooking oil biodiesel [24]. These studies consistently report that hydrogen enrichment improves brake thermal efficiency and lowers HC/CO emissions, while tending to increase NO_x, in line with the classical thermal-NO trade-off. Dual-fuel operation with cottonseed oil and hydrogen has also been analyzed with varying injection opening pressures [30] and higher hydrogen flow rates in CRDI engines [31]. The present investigation is broadly consistent with these qualitative trends but adds two specific contributions: (i) it focuses on a cottonseed B20-hydrogen strategy at 75% load and demonstrates a balanced operating point (IP = 240 bar, CR = 17.5, H_2 = 10 L/min) where BTE (33.52%), HC (65 ppm) and CO (0.016%) are jointly improved relative to the B20 baseline while NO_x remains within the expected dual-fuel range; and (ii) it introduces a hybrid Entropy-VIKOR-Taguchi framework that simultaneously prioritizes emissions and combustion indicators and quantifies the relative importance of NO_x, HC, CO, BTE and combustion metrics in the compromise solution. This provides a more explicit, data-driven, sustainability-oriented optimization than in earlier hydrogen-biodiesel studies, where parameter tuning was typically single-objective or based solely on RSM or ANN approaches.

4. Conclusions

This study presented a new hybrid Entropy-VIKOR-Taguchi model to optimize the performance, combustion, and emission parameters of a diesel engine operating on a cottonseed biodiesel (B20)-hydrogen dual-fuel blend. It advances dual-fuel diesel optimization by introducing a single, reproducible decision protocol that converts a multi-response sustainability problem into an objective compromise solution. The key contribution is the coupling of entropy-derived response weights with VIKOR compromise ranking inside a Taguchi design, which removes subjective prioritization of emissions versus performance and yields a defendable "best trade-off" operating point rather than a collection of disconnected optima. Some of the key conclusions that can be drawn are:

(i) The dual-fuel strategy (B20 + H_2) achieved a Brake Thermal Efficiency (BTE) of up to 33.52% and a minimum Brake Specific Fuel Consumption (BSFC) of 0.213 kg/kWh, representing a notable efficiency improvement over baseline diesel operation.

(ii) Hydrogen enrichment promoted faster combustion and higher in-cylinder pressures, with peak pressure reaching 85 bar and a maximum Heat Release Rate (HRR) of 86 J/deg, thereby enhancing power output.

(iii) Emission analysis revealed a minimum HC of 65 ppm and a CO level of 0.016%, both significantly lower than those of conventional diesel, confirming superior oxidation and atomization at optimized injection pressures.

(iv) However, NO_x emissions peaked at 1380 ppm under high hydrogen flow, highlighting the classic trade-off between efficiency and emissions and the importance of precise parameter optimization.

(v) Entropy weighting ranked NO_x as the most sensitive parameter (weight = 0.1638), underscoring its dominant role in sustainability-oriented optimization.

(vi) VIKOR-ANOVA analysis confirmed injection pressure (42.5% contribution) as the most influential factor, followed by compression ratio (28.07%) and hydrogen flow rate (15.63%).

(vii) The optimal operating condition, IP = 240 bar, CR = 17.5, H_2 = 10 L/min, provided the best compromise solution with the lowest VIKOR index (Q = 0.0588), balancing performance gains with emission reductions.

The optimization is based on an L9 orthogonal array at a single engine speed and 75% load, so only main effects are well captured, and higher-order interactions or strong response curvature may not be fully resolved. Future studies should therefore employ extended experimental designs (e.g., RSM or larger factorial/Taguchi arrays) across multiple speeds and loads. The hybrid decision-making framework proposed has demonstrated the ability to achieve strong trade-offs across several objectives, opening the possibility of operating diesel engines in dual-fuel mode in a sustainable manner. This research provided a computationally efficient and reproducible protocol for experimental engine optimization by integrating entropy-based weighting and VIKOR compromise ranking into a Taguchi design. Although the current study confirms the framework of cottonseed bio-diesel and hydrogen blends under controlled laboratory under controlled laboratory conditions, future studies must extend the framework to transient duty cycles, include the strategy of advanced after-treatment to reduce the peak of NO_x, evaluate the long-term durability effects on the engine hardware, and incorporate the emerging forms of alternative fuels like e-fuels, ammonia, or bio-alcohols in the hybrid multi-fuel systems.

Acknowledgements

The authors thank the Department of Mechanical Engineering, Vidya Jyothi Institute of Technology, Aziznagar, Hyderabad, India, for providing the laboratory facilities that enabled this work.

Funding

This study was not supported by any grants from funding bodies in the public, private, or not-for-profit sectors.

Declaration of Competing Interest
The author declares no conflicts of interest.

CRediT Authorship Contribution Statement
N. Khan (Conceptualization; Methodology; Writing - original draft)
J.K. Jatavallabhula (Validation; Formal analysis; Data curation; Writing - original draft)
P. Bridjesh (Investigation; Resources; Software)
V.V. Satyanarayana (Writing - review & editing; Project administration; Supervision)

Availability of Data and Materials
The data supporting this study's findings are available on request from the corresponding author.

Ethics Declarations
This study did not involve human participants or animals. Ethical approval was therefore not required.

Generative Artificial Intelligence Declarations
The authors stated that generative AI was not used to generate content, ideas, or theories. We have just utilized AI to enhance readability and refine the language. This was used with extreme human control and oversight. The authors take full responsibility for reviewing and approving the content.

References
[1] C. Caraveo Mena, J.A. Suastegui Macias, L. Cervantes Huerta, J.A. Ruiz Ochoa, S. Jiménez Calleros, A. Sánchez-Pérez, "Design and implementation of a distributed IoT system for monitoring of gases emitted by vehicles that use biofuels," *Sustainability,* vol. 17, no. 3, p. 1153, 2025.
[2] D. Xu, H. Yu, W. Cai, J. Xu, J. Li, "Primary particulate matter and aerosol emissions from biodiesel engines during idling in plateau environments of China," *Sustainability,* vol. 17, no. 3, p. 976, 2025.
[3] J. Syed, "Significant research on sustainable oxygenated fuel for compression ignition engines with controlled emissions and optimum performance prediction using artificial neural network," *Sustainability,* vol. 17, no. 2, p. 788, 2025.
[4] P. Chen, J. Fang, Z. Zuo, C. Zhang, K. Wang, Z. Han, et al., "A review of perovskite catalysts for the simultaneous elimination of soot and nox emissions from diesel engine," *Sustainability,* vol. 16, no. 23, p. 10793, 2024.
[5] D. Firoiu, G.H. Ionescu, C.M. Cismaș, M.P. Costin, L.M. Cismaș, Ș.C.F. Ciobanu, "Sustainable production and consumption in eu member states: achieving the 2030 sustainable development goals (SDG 12)," *Sustainability,* vol. 17, no. 4, p. 1537, 2025.
[6] M. Jakubowski, A. Jaworski, H. Kuszewski, K. Balawender, "Performance of a diesel engine fueled by blends of diesel fuel and synthetic fuel derived from waste car tires," *Sustainability,* vol. 16, no. 15, p. 6404, 2024.
[7] S.S. Almady, A.I. Moussa, M.M. Deef, M.F. Zayed, S.M. Al-Sager, A.M. Aboukarima, "Biodiesel production through the transesterification of non-edible plant oils using glycerol separation technique with a high voltage," *Sustainability,* vol. 16, no. 7, p. 2896, 2024.
[8] M. Fratita, R.M. Chivu, E. Rusu, G.B. Carp, I. Ion, F.P. Brito, "Experimental investigation of methyl ester–ethanol blends as a sustainable biofuel alternative for heavy duty engines," *Sustainability,* vol. 17, no. 1, p. 253, 2025.
[9] A. Alatawneh, A. Torok, "Projecting AV sales in the EU-27 and UK: Insights from Euro emission standards and historical trends," *Transport Policy,* vol. 163, pp. 91-101, 2025.
[10] T. Mizik, "European Union guidelines for the production of different generations of biofuels," in *Biofuels and Sustainability*: Elsevier, 2025, pp. 205-219.
[11] K. Liang, J. Liang, G. Li, Z. Shao, Z. Jiang, J. Feng, "Improvement of engine combustion and emission characteristics by fuel property modulation," *Sustainability,* vol. 16, no. 23, p. 10764, 2024.
[12] J. M. Rueda-Vázquez, J. Serrano, S. Pinzi, F.J. Jiménez-Espadafor, M. Dorado, "A review of the use of hydrogen in compression ignition engines with dual-fuel technology and techniques for reducing NOx emissions," *Sustainability,* vol. 16, no. 8, p. 3462, 2024.
[13] W. Gu, W. Su, "Study on the effects of exhaust gas recirculation and fuel injection strategy on transient process performance of diesel engines," *Sustainability,* vol. 15, no. 16, p. 12403, 2023.
[14] S. Ellappan, B. Pappula, "Utilization of unattended waste plastic oil as fuel in low heat rejection diesel engine," *Sustainable Environment Research,* vol. 29, no. 1, p. 2, 2019.
[15] J. Žaglinskis, A. Rimkus, "Research on the performance parameters of a compression-ignition engine fueled by blends of diesel fuel, rapeseed methyl ester and hydrotreated vegetable oil," *Sustainability,* vol. 15, no. 20, p. 14690, 2023.
[16] S. Vellaiyan, "Optimization of hydrogen-enriched biodiesel-diesel dual-fuel combustion with EGR for sustainable engine performance," *International Journal of Hydrogen Energy,* vol. 128, pp. 85-94, 2025.
[17] S. Seetharaman, P.V. Kumar, S. Thiagarajan, G. Dhamodaran, M. Vikneswaran, A.R. Raj, et al., "Combustion, performance, and emission analysis of hydrogen-enhanced diesel blends with Scenedesmus dimorphus biodiesel:

A third-generation biofuel study," *International Journal of Hydrogen Energy,* vol. 155, p. 150312, 2025.

[18] A. Shirneshan, B. Kanberoglu, G. Gonca, "Experimental investigation and parametric modeling of the effect of alcohol addition on the performance and emissions characteristics of a diesel engine fueled with biodiesel-diesel-hydrogen fuel mixtures," *Fuel,* vol. 381, p. 133489, 2025.

[19] D. Li, S. Devanesan, T. Kim, K. Brindhadevi, "Enhanced combustion performance and emission reduction in diesel engines fuelled by microalgae biodiesel blends with TiO_2 nanoparticles and hydrogen-rich biogas," *International Journal of Hydrogen Energy,* vol. 185, p. 151933, 2025.

[20] S.K. Nayak, P.C. Mishra, S. Nanda, Y. Devarajan, "Impacts of organic antioxidant additive on the performance and emission characteristics of a diesel engine fuelled with hydrogen-biodiesel blends in dual-fuel mode," *International Journal of Hydrogen Energy,* vol. 127, pp. 930-944, 2025.

[21] C. Selvam, Y. Devarajan, A.K. Dash, S. Saxena, B. Nagappan, V.K. Singh, et al., "Improving diesel engine performance with hydrogen-fumigated soapnut biodiesel," *Results in Engineering,* p. 106287, 2025.

[22] K. Bayramoğlu, T. Bayramoğlu, F. Polat, S. Sarıdemir, N. Alçelik, Ü. Ağbulut, "Energy, exergy, and emission (3E) analysis of hydrogen-enriched waste biodiesel-diesel fuel blends on an indirect injection dual-fuel CI engine," *Energy,* vol. 314, p. 134124, 2025.

[23] G.L. Leo, R. Jayabal, A. Kathapillai, S. Sekar, "Performance and emissions optimization of a dual-fuel diesel engine powered by cashew nut shell oil biodiesel/hydrogen gas using response surface methodology," *Fuel,* vol. 384, p. 133960, 2025.

[24] S. Thiagarajan, S. Seetharaman, R. Lokesh, G. Prasanth, B. Karthick, J.S.F. Josephin, et al., "Impact of hydrogen-assisted combustion in a toroidal re-entrant combustion chamber powered by rapeseed oil/waste cooking oil biodiesel," *International Journal of Hydrogen Energy,* vol. 104, pp. 367-377, 2025.

[25] S. Srinivasan, B. Musthafa, B.V.V. Naidu, M.S. Kumar, "Optimization and experimental investigation on CI engine characteristics fuelled with low carbon alcohols and juliflora biodiesel blends: A RSM approach," *Fuel,* vol. 388, p. 134542, 2025.

[26] D. Ning, J. Dong, W. Guan, Z. Wang, H. Wang, T. Lin, et al., "Experimental analysis and multi-objective optimization of heavy-duty hydrogen SI engine performance and emissions based on GA-BP-MOGWO," *Energy Conversion and Management,* vol. 329, p. 119638, 2025.

[27] H. Venu, M.E.M. Soudagar, T.S. Kiong, N.M. Razali, H.R. Wei, T.M.Y. Khan, et al., "Performance and emission prediction using ANN (artificial neural network) on H2-assisted Garcinia gummi-gutta biofuel doped with nano additives," *Scientific Reports,* vol. 15, no. 1, p. 5911, 2025.

[28] A. Baluchamy, M. Saravanamuthu, S.S. Natarajan, S.R. Chandramurthy, "Analysis of energy, exergy, and emissions in a diesel engine powered by cotton silk seed oil biodiesel with varying injection timings," *Environmental Science and Pollution Research,* pp. 1-15, 2025.

[29] A. El-Shafay, Ü. Ağbulut, S. Shanmugan, M. Gad, "Production of oxy-hydrogen with an alkaline electrolyzer, and its impacts on engine behaviors fuelled with diesel/waste fish biodiesel mixtures supported by graphene nanoparticles," *Energy,* vol. 314, p. 133934, 2025.

[30] S. Yousufuddin, E.N. Mahrous, M. Saleem, "Experimental analysis of hydrogen addition at varying injection opening pressures on a dual-fuel diesel engine operating with diesel and cottonseed oil," *Arabian Journal for Science and Engineering,* vol. 50, no. 12, pp. 9291-9305, 2025.

[31] V. Gnanamoorthi, V. Vimalananth, "Effect of hydrogen fuel at higher flow rate under dual fuel mode in CRDI diesel engine," *International Journal of Hydrogen Energy,* vol. 45, no. 33, pp. 16874-16889, 2020.

[32] I.S. Mohamed, E.P. Venkatesan, M. Parthasarathy, S.R. Medapati, M. Abbas, E. Cuce, et al., "Optimization of performance and emission characteristics of the CI engine fueled with preheated palm oil in blends with diesel fuel," *Sustainability,* vol. 14, no. 23, p. 15487, 2022.

[33] J. Anta, "How to Conceptual Engineer 'Entropy ' and 'Information'," *Erkenntnis,* pp. 1-25, 2025.

[34] V. Hariram, R. Sathishbabu, J. Godwin John, K. Vijayakumar, E. Sangeeth Kumar, K. Kamakshi Priya, "Enhanced combustion and emission characteristics of diesel-algae biodiesel-hydrogen blends in a single-cylinder diesel engine," *Results in Engineering,* vol. 26, p. 104676, 2025.

[35] R. Jayabal, "Environmental impact of adding hybrid nanoparticles and hydrogen to the algae biodiesel-diesel blend on engine emissions," *Process Safety and Environmental Protection,* vol. 198, p. 107102, 2025.

[36] G.N. Kannaiyan, B. Pappula, S. Makgato, "Experimental investigation on addition of furfuryl alcohol to diesel plastic fuel blends and optimization using Kissing Numbers," *Scientific Reports,* vol. 15, no. 1, p. 20672, 2025.

[37] K. Gupta, N. Singh, P. Goswami, A. Priyam, "Energy and exergy analysis of diesel engine fuelled with hydrogen and Algae Oil as secondary fields," *International Journal of Hydrogen Energy,* vol. 163, p. 150712, 2025.

[38] S. Tandon, R. Kacker, S. Singh, S. Gautam, S.K. Tamang, "Multi-objective optimization of mechanical properties of additively manufactured tri-hexagon pattern specimens using machine learning algorithms," *Progress in Additive Manufacturing,* vol. 10, no. 5, pp. 3659-3672, 2025.

[39] S. Kanth, T. Ananad, S. Debbarma, B. Das, "Effect of fuel opening injection pressure and injection timing of hydrogen-enriched rice bran biodiesel fuelled in CI engine," *International Journal of Hydrogen Energy,* vol. 46, no. 56, pp. 28789-28800, 2021.

[40] Harshalatha, S. Patil, P.G. Kini, "A review on simulation-based multi-objective optimization of space layout design parameters on building energy performance," *Journal of Building Pathology and Rehabilitation,* vol. 9, no. 1, p. 69, 2024.

[41] L.R. Kunchi, S.K. Bhatti, S.V.P. Lankapalli, J. Sagari, "Effect of multi-ferrite nanoparticles added Terminalia bellirica biodiesel on diesel engine: combustion, performance, and emission studies," *International Journal of Thermofluids,* vol. 22, p. 100652, 2024.

[42] F. Okumuş, B. Kanberoğlu, G. Gonca, G. Kökkülünk, Z. Aydın, C. Kaya, "The effects of ammonia addition on the emission and performance characteristics of a diesel engine with variable compression ratio and injection timing," *International Journal of Hydrogen Energy,* vol. 64, pp. 186-195, 2024.

[43] M. Kolli, C. Sunnapu, N.R. Medikondu, "Multi-response optimization of friction stir welding process parameter of AA 5083 with Taguchi-VIKOR approach," *Journal of Engineering and Applied Science,* vol. 72, no. 1, p. 2, 2025.